American Journal of Pathology, Vol. 165, No. 2, August 2004
Copyright © American Society for Investigative Pathology

Insulin-Like Growth Factor-I Plays a Pathogenetic Role in Diabetic Retinopathy

Vassiliki Poulaki,* Antonia M. Joussen,†‡ Nicholas Mitsiades,§ Constantine S. Mitsiades,§ Eirini F. Iliaki,* and Anthony P. Adamis*¶

From the Retina Research Institute, Massachusetts Eye and Ear Infirmary, and the Department of Adult Oncology,§ Dana-Farber Cancer Institute, Harvard Medical School, Boston, Massachusetts; the Eyetech Research Center,¶ Eyetech Pharmaceuticals, Woburn, Massachusetts; and the Department of Vitreoretinal Surgery,† Center of Ophthalmology, and Zentrum für Molekulare Medizin Köln,‡ the Center for Molecular Medicine University of Cologne, Cologne, Germany*

Diabetic retinopathy is a leading cause of blindness in the Western world. Aberrant intercellular adhesion molecule-1 expression and leukocyte adhesion have been implicated in its pathogenesis, raising the possibility of an underlying chronic inflammatory mechanism. In the current study, the role of insulin-like growth factor (IGF)-I in these processes was investigated. We found that systemic inhibition of IGF-I signaling with a receptor-neutralizing antibody, or with inhibitors of PI-3 kinase (PI-3K), c-Jun kinase (JNK), or Akt, suppressed retinal Akt, JNK, HIF-1α, nuclear factor (NF)-κB, and AP-1 activity, vascular endothelial growth factor (VEGF) expression, as well as intercellular adhesion molecule-1 levels, leukostasis, and blood-retinal barrier breakdown, in a relevant animal model. Intravitreous administration of IGF-I increased retinal Akt, JNK, HIF-1α, NF-κB, and AP-1 activity, and VEGF levels. IGF-I stimulated VEGF promoter activity *in vitro*, mainly via HIF-1α, and secondarily via NF-κB and AP-1. In conclusion, IGF-I participates in the pathophysiology of diabetic retinopathy by inducing retinal VEGF expression via PI-3K/Akt, HIF-1α, NF-κB, and secondarily, JNK/AP-1 activation. Taken together, these *in vitro* and *in vivo* signaling studies thus identify potential targets for pharmacological intervention to preserve vision in patients with diabetes. *(Am J Pathol 2004, 165:457–469)*

Although the molecular pathophysiology of diabetic retinopathy, the current leading cause of blindness in Western societies,[1] is not fully elucidated, studies have documented a pivotal role for leukocyte adherence within the retinal vasculature. The adhesion of leukocytes to the retinal endothelium is a process that depends on β_2 integrin-intercellular adhesion molecule (ICAM)-1 interactions and leads to breakdown of the blood-retinal barrier.[2] These data, in combination with our previous findings that aggressive anti-inflammatory therapy suppressed leukocyte adhesion and blood retinal breakdown in a relevant animal model,[3] support the hypothesis that a chronic subclinical inflammation may underlie much of the vascular pathology of diabetic retinopathy.[4] These vascular pathological findings are orchestrated by vascular endothelial growth factor (VEGF), a factor that potently promotes the growth and maintenance of endothelial cells and the formation of new vessels, and is implicated in both background and proliferative diabetic retinopathy.[5–11] Intraocular VEGF levels are increased in diabetic patients with blood-retinal barrier breakdown and neovascularization,[5,10,12,13] whereas the specific inhibition of VEGF prevents these complications in animal models.[7,11,14] Therefore, regulation of VEGF expression could conceivably be both a mediator for converging local and systemic stimuli modulating vessel pathophysiology, as well as a target for therapeutic intervention. Within a constellation of known modulators of VEGF expression that can possibly function at the transcriptional [through AP-1, AP-2, steroid hormone receptors, p53, and nuclear factor (NF-κB)] or posttranscriptional level,[15–18] hypoxia is the most potent inducer of VEGF transcription *in vivo*; its effects are mainly mediated by the helix-loop helix (bHLH)-PAS transcription factor HIF-1α, which heterodimerizes with the bHLH-PAS protein ARNT or HIF-1β,[19–22] and binds to consensus and ancillary hypoxia-response elements (HREs) in the VEGF promoter.[21,23–25]

Yet, aside from hypoxia, additional factors may also regulate VEGF expression *in vivo*. Insulin-like growth factor (IGF)-I is one such candidate: vitreous IGF-I levels correlate with the presence and severity of ischemia-associated diabetic retinal neovascularization;[26] intravitreal IGF-I injection dose-dependently causes retinal neovascularization and microangiopathy;[27] whereas reduction of serum IGF-I levels

Supported by the Roberta W. Siegel Fund (to A.P.A.), the Foundation Fighting Blindness (to V.P.), the National Institutes of Health (EY12611 and EY11627 to A.P.A.), the Juvenile Diabetes Foundation (to A.P.A., A.M.J.), the Falk Foundation (to A.P.A.), the Iaccoca Foundation (to A.P.A.), and the Center for Molecular Medicine University of Cologne (ZMMK) Deutsche Forschungsgemeinschaft (DFG Jo 324/4-1 to A.M.J.).

V.P. and A.M.J. contributed equally in this work.

Accepted for publication April 8, 2004.

Address reprint requests to Anthony P. Adamis, M.D., Eyetech Research Center, 42 Cummings Park, Woburn, MA 01801. E-mail: tony.adamis@eyetk.com.

inhibits retinal neovascularization in an ischemic murine model.[28] Pituitary ablation acutely improved visual acuity and suppressed proliferative diabetic retinopathy in some diabetic retinopathy patients, raising the hypothesis that decreases in growth hormone and IGF-I underlie this phenomenon.[29,30] Of note, proliferative diabetic retinopathy is rare in dwarfs who are deficient in growth hormone and IGF-I.[31] Importantly, recombinant IGF-I exacerbated diabetic retinopathy, when administered to diabetic patients in an attempt to suppress growth hormone secretion and reverse insulin resistance.[32,33]

Despite these indications, however, direct proof of the precise role of IGF-I in the development and progression of diabetic retinopathy is lacking, and the signaling pathway(s) mediating its actions have not been delineated. We have previously demonstrated that IGF-I potently increases VEGF expression in retinal pigment epithelial (RPE) cells *in vitro* and has an additive effect with hypoxia *in vivo*.[34] We now report that IGF-I directly participates in the pathophysiology of diabetic retinopathy by increasing VEGF expression via a PI-3K/Akt-dependent mechanism that involves HIF-1α and NF-κB/AP-1. We also identify a constellation of molecular targets in the IGF-I-induced signaling cascades that can potentially be used in new therapeutic strategies for diabetic retinopathy.

Materials and Methods

Cell Culture

Human RPE cells (passage 2) were a generous gift of Dr. B. Kirchhof (University of Cologne, Cologne, Germany). Previous work has shown that these cells recapitulate retinal VEGF regulation *in vivo*.[18,34–36] The NF-κB subunit RelA$^{+/+}$ and RelA$^{-/-}$ 3T3 fibroblasts were a generous gift from Dr. D. Baltimore (Massachusetts Institute of Technology, Cambridge, MA).[37] We maintained all cells in Dulbecco's modified essential medium (DMEM; Sigma, St. Louis, MO) containing 10% heat-inactivated fetal calf serum (Hyclone Laboratories, Logan, UT) and 100 U/ml penicillin, 100 mg/ml streptomycin, and 2 mmol/L L-glutamine. Cells were plated onto six-well plastic plates and used for experiments when they reached 80 to 100% confluence. Cells were cultured in fresh serum-free media for 12 hours before experiments. The PI-3K inhibitors wortmannin and LY294002, the Hsp90 chaperone inhibitor geldanamycin and the c-Jun kinase (JNK) inhibitors I and II (SP600125) were purchased from Calbiochem (La Jolla, CA). The NF-κB inhibitor SN50 was purchased from Biomol (Plymouth Meeting, PA). After a 1-hour preincubation with the various inhibitors (at concentrations of 50 μmol/L, except wortmannin, which was used at a concentration of 50 nmol/L), we performed 12-hour incubations with 100 ng/ml of recombinant IGF-I (R&D Systems, Minneapolis, MN). The inhibitors were free of toxicity at the concentration and for the period of time they were used. Each condition was prepared in triplicate, and we performed the experiments at least three times with reproducible results. Representative experiments are shown in the figures.

Plasmids

The eukaryotic expression vector pXP2 carrying 1.7 kb of VEGF gene 5′ flanking sequence (*Eco*RV-*Pst*I) 5′ to the luciferase gene, as well as deletion mutants that carry 1.0 kb, 0.8 kb, 0.5 kb, and 0.1 kb from the human VEGF promoter (1.0 pXP2, 0.8 pXP2, 0.5 pXP2, and 0.1 pXP2, respectively) have been previously described.[24] The plasmid pT81-luc contains 81 bp of the thymidine kinase minimum promoter constructed 5′ to the luciferase gene of the pXP2 expression vector. The pUSEamp vector containing the cDNAs for constitutively active Akt (aAkt) and dominant-negative (DN) Akt, respectively, was purchased from Upstate Biotechnologies (Lake Placid, NY). The plasmid containing a segment of rat VEGF cDNA containing exons 4 through 7 and a portion of exon 8 was previously described.[34]

Transient Transfection

For transient transfections, we plated cells (10^6) in 100 cm^2 tissue culture-treated Petri dishes and transfected with 1 μg of the vector expressing constitutively active Akt or DN-Akt, or HIF-1a anti-sense or sense oligonucleotides, with the Superfect reagent (Qiagen, Valencia, CA). Twenty-four hours after transfection, the cells transfected with the activated form of Akt were washed with Hanks' balanced salt solution and harvested. The cells transfected with the DN-Akt, the sense, and anti-sense HIF-1a oligonucleotides were serum-starved for 6 hours and incubated overnight with 100 ng/ml of IGF-I in serum-free media. Cell extracts were prepared the following day for enzyme-linked immunosorbent assay (ELISA), as described in subsequent sections.

Reporter Assays

For transient transfections, 5×10^5 cells/well were plated in 12-well plates, transfected with 1 μg of the reporter construct DNA with the Superfect reagent (Qiagen) and harvested 24 hours later. Cell extracts were prepared by using the reporter lysis buffer (Promega, Madison, WI) and luciferase activity was measured with the luciferase assay kit (Promega) according to the manufacturer's instructions. Transfection efficiencies were normalized by co-transfecting 1 μg of a β-galactosidase construct followed by quantification of β-galactosidase expression using β-galactosidase activity assay kit (Boehringer Mannheim, Indianapolis, IN) according to the instructions of the manufacturer. For normalization, the luciferase activity values were divided by the β-galactosidase values.

Animals and Experimental Diabetes

All animal experiments were performed according to the guidelines of the Association for Research in Vision and Ophthalmology and were approved by the Animal Care and Use Committees of the Boston Children's Hospital and Massachusetts Eye and Ear Infirmary. Male Long-Evans rats weighing ~200 g (Charles River Laboratories,

Wilmington, MA) received a single 60 mg/kg injection of streptozotocin (Sigma, St. Louis, MO) in 10 mmol/L citrate buffer, pH 4.5, after an overnight fast. Control nondiabetic rats received injections of citrate buffer alone. Twenty-four hours later, rats with blood glucose levels greater than 250 mg/dl were deemed diabetic. The animals were then assigned to their various treatment groups in a randomized manner. All rat experiments were performed 2 weeks after the induction of diabetes. All animals were fed standard laboratory chow and were allowed free access to food and water in an air-conditioned room with a 12-hour light/dark cycle. The weight of the animals had a range between 180 to 220 g and their blood glucose was between 250 to 350 mg/dl.

Intravitreal Injections

Intravitreous injections were performed by inserting a 30-gauge needle into the vitreous of anesthetized Long-Evans rats at a site 1-mm posterior to the limbus of the eye. Insertion and infusion were performed and directly viewed through an operating microscope. Care was taken not to injure the lens or the retina. The tip of the needle was positioned over the optic disk and a 5-μl volume was slowly injected into the vitreous. Any eyes that exhibited damage to the lens or retina were discarded and not used for the analyses.

Implantation of the Osmotic Pumps

To achieve steady drug levels in the circulation of animals, drugs were administered by slow intraperitoneal release from osmotic pumps instead of repeated intraperitoneal injections. One day after the induction of diabetes, osmotic pumps (Alzet, Cupertino, CA) were implanted as previously described.[38] We used the following inhibitors: wortmannin and LY294002 (PI-3K inhibitors), the aIR-3 monoclonal antibody (which specifically neutralizes the activity of the human and mouse IGF receptor I[39]) (Oncogene Research, Cambridge, MA), Jun kinase (JNK) inhibitor I and JNK inhibitor II (SP600125), the SN50 peptide inhibitor of NF-κB nuclear translocation and transcriptional activity, and lastly, geldanamycin, which specifically inhibits the hsp90 molecular chaperone and depletes the intracellular levels of several kinases, including Akt. The dose of the various inhibitors chosen in the current study was titrated in previously performed dose-response experiments.[38] The various inhibitors were also tested in normal (nondiabetic) rats with no significant effect on the variables tested (data not shown). The effect of the IGFR-neutralizing antibody was compared to that of an isotype-matched control, whereas that of the small molecule inhibitors to administration of vehicle alone. Two hundred μg of each inhibitor were inserted in each osmotic pump, which releases 0.5 μg/hour for 7 days.

Measurement of Blood-Retinal Barrier Breakdown Using Evans Blue

Blood-retinal barrier breakdown was measured in 2-week diabetic animals using Evans blue dye as described previously.[40] Blood-retinal barrier breakdown was calculated using the following equation, with results being expressed in μl plasma $\times$ g retina dry weight^{-1} $\times$ hour^{-1}.

$$\frac{\text{Evans blue } (\mu\text{g})/\text{retina dry weight (g)}}{\text{Time-averaged Evans blue concentration } (\mu\text{g/plasma}\mu\text{l})/\text{circulation time (hr)}}$$

VEGF and IGF-I ELISA

Retinal lysates from six animals (12 eyes in total) were used for each ELISA assay. Each retina was placed in 200 μl of lysis buffer [20 mmol/L imidazole HCl, 10 mmol/L KCl, 1 mmol/L $MgCl_2$, 10 mmol/L EGTA, 1% Triton, 10 mmol/L NaF, 1 mmol/L Na molybdate, 1 mmol/L ethylenediaminetetraacetic acid (EDTA), pH 6.8] supplemented with a protease inhibitor cocktail (Boehringer Mannheim) followed by sonication. The lysate was cleared of debris by centrifugation at 10,000 $\times$ *g* for 15 minutes (4°C), and the supernatant was assayed. Total protein was determined using the BCA kit (Bio-Rad, Hercules, CA). VEGF and IGF-I levels in retinal supernatants were determined using the respective sandwich ELISAs according to the manufacturer's instructions (R&D Systems) and normalized to total protein. In the case of IGF-I, samples were pretreated according to the manufacturer's instructions to release IGF-I from binding proteins. The minimum detectable levels for VEGF and IGF-I with these assays are 5 pg/ml and 26 pg/ml, respectively.

Preparation of Nuclear Extracts

Pooled retinae from nondiabetic and diabetic rats (three in each group) were isolated and homogenized as previously described.[38] Briefly, retinae were homogenized with a mechanical homogenizer in five pellet volumes of buffer A [20 mmol/L Tris, pH 7.6, 10 mmol/L KCl, 0.2 mmol/L EDTA, 20% (by volume) glycerol, 1.5 mmol/L $MgCl_2$, 2 mmol/L dithiothreitol, 1 mmol/L Na_3VO_4, and protease inhibitors; Roche Molecular Biochemicals Inc., Indianapolis, IN]. The nuclei were pelleted (2500 $\times$ *g*, 10 minutes) and resuspended in two pellet volumes of buffer B (identical to buffer A except that KCl was increased to 0.42 mol/L). Nuclear debris was removed by centrifugation (15,000 $\times$ *g*, 20 minutes), and the supernatant was dialyzed against one exchange of buffer Z (20 mmol/L Tris-HCl, pH 7.8, 0.1 mol/L KCl, 0.2 mmol/L EDTA, 20% glycerol) for at least 3 hours at 4°C with Dialyze Z cassettes (Pierce Co., Rockford, IL). The protein concentration was measured using a Pierce assay with serum albumin as a standard.

Electrophoretic Mobility Shift Assay

Oligonucleotide probes (Life Technologies, Inc., Rockville, MD) containing the HIF-1α-binding and ancillary HIF-1α-binding sites were biotinylated by 5′ end labeling of the sense strand with biotin-dUTP using T4 polynucleotide kinase (Roche Diagnostics, Indianapolis, IN). The binding reactions were done in a volume of 20 μl containing 5 μg of nuclear extracts and 0.1 μg of denatured calf thymus DNA in 10 mmol/L Tris-HCL (pH 7.5), 50 mmol/L KCL, 50 mmol/L NaCl, 1 mmol/L $MgCl_2$, 1 mmol/L EDTA, 5 mmol/L dithiothreitol, and 5% glycerol for 30 minutes on ice, and in the case of the supershift experiment, an additional 20-minute incubation at 4°C. The mouse monoclonal anti-HIF-1α (Alexis Biochemicals, San Diego, CA), and the rabbit polyclonals anti-NF-κB and anti-c-Jun (Santa Cruz, Santa Cruz, CA) were used for the supershift experiments. For the competition experiments, competitor DNA was added 5 minutes before the addition of the labeled probe. The reaction mixture was then loaded onto a 5% nondenaturing polyacrylamide gel, which was prerun at 185 V for 2 hours. Electrophoresis was performed at 185 V in 0.3× TBE (26.7 mmol/L boric acid and 1.5 mmol/L EDTA) at 4°C. The gels were transferred onto a positively charged nylon membrane (Biodyne A, Pierce), and incubated with a stable streptavidin-horseradish peroxidase conjugate. The horseradish peroxidase reaction was developed with the Opti4CN substrate reagent (Biomol).

Quantification of NF-κB and AP-1 Activation

NF-κB and AP-1 activation was analyzed using the *Trans*-AM NF-κB and *Trans*-AM c-jun transcription factor assay kit (Active Motif, Carlsbad, CA) according to the manufacturer's instructions, as previously described.[41,42] The nuclear extracts were incubated in 96-well plates coated with immobilized oligonucleotides containing consensus binding sites for the respective transcription factors. Transcription factor binding to the target oligonucleotide was detected by incubation with respective specific primary monoclonal antibodies, visualized by anti-IgG horseradish peroxidase conjugate and developing solution, and quantified at 450 nm with a reference wavelength of 655 nm. Background binding was calculated by adding in selected wells the respective consensus oligonucleotides in excess (20 pmol/well) as soluble competitors that prevented transcription factor binding to the probe immobilized on the plate. The resulting values were subtracted from the values obtained in wells with immobilized oligonucleotides alone. The ELISA format of this assay allowed for repeated measurements of each specimen and resulted in high sensitivity and reproducibility. For the NF-κB and AP-1 transcription factor assays six animals were used from each group and retinas were not pooled.

Binding Assays for HIF-1α

The HIF-1α-binding site and the HIF-1α ancillary-binding site that exists in the VEGF promoter (sequence) was added at the 3′ end of a 100-bp random sequence chosen for the absence of the HIF-1 consensus sequence. The resulting 122-bp probe was produced by polymerase chain reaction using a biotinylated forward primer and for the reverse primer the HIF-1α-binding sequence. The polymerase chain reaction product was purified on ultracentrifugation membranes. The 5′ extremity of the probe is biotinylated and was linked to streptavidin-coated 96-well plates (Roche Diagnostics): 2 pmol of probe per well were incubated for 1 hour at 37°C in 50 μl of phosphate-buffered saline (PBS). Plates were subsequently washed to remove the excess probe. Fifty μl of binding buffer were subsequently incubated with 20 μl of nuclear extracts in the wells coated with the probe, for 1 hour at room temperature with mild agitation. The wells were subsequently washed with PBS supplemented with 0.1% Tween-20 and were incubated with a monoclonal antibody against HIF-1α (Alexis Biochemicals) at a 1/1000 dilution in PBS with 1% nonfat dried milk, for 1 hour at room temperature. After washes the wells were incubated with a peroxidase-conjugated anti-mouse antibody (Southern Biotechnologies, Birmingham, AL) at a 1/1000 dilution in PBS with 1% nonfat dried milk, for 1 hour at room temperature. The peroxidase reaction was developed with tetramethylbenzidine (100 μl; Biosource, Camarillo, CA) that was incubated for 10 minutes at room temperature, it was stopped with 100 μl of stop solution (Biosource), and it was read at 450 nm. For the HIF-1a transcription factor assay six animals were used from each group and retinas were not pooled.

Measurement of Retinal Akt-Kinase Activity

Retinal Akt kinase activity was quantified using a modified ELISA protocol as previously described.[43] The peroxidase reaction was developed and measured at 450 nm with a reference wavelength at 620 nm.

Measurement of Retinal JNK Activity

Retinal jun kinase activity was quantified using a modified ELISA protocol. Briefly, each well of a 96-well microtiter plate was coated with 100 μl of 1 μmol/L c-Jun fusion protein, which serves as a substrate for the activated Jun kinase, overnight at 4°C in carbonate buffer (15 mmol/L Na_2CO_3, 35 mmol/L $NaHCO_3$, 0.2 g/L NaN_3, pH 9.6). After washing, the remaining active sites were blocked in 10 mg/ml of bovine serum albumin in PBS containing 0.05% Tween-20. Whole retinae were dissected from treated animals as described above and homogenized in lysis buffer containing 20 mmol/L Tris (pH 7.5), 150 mmol/L NaCl, 1 mmol/L EDTA,1 mmol/L EGTA, 1% Triton X-100, 2.5 mmol/L sodium pyrophosphate, 1 mmol/L glycerolphosphate, 1 mmol/L Na_3O_4, 1 μg/ml leupeptin, 1 mmol/L phenylmethyl sulfonyl fluoride. The lysates were cleared by centrifugation and protein was quantified with the BCA assay. The jun kinase was precipitated from 100 μl of lysate from each condition with the addition of 15 μl of immobilized Jun fusion protein (Cell Signaling Technology, Beverly, MA) overnight at 4°C and incubated with the c-Jun fusion protein in kinase buffer (25 mmol/L Tris, pH 7.5, 5 mmol/L glycerolphosphate, 2 mmol/L dithiothreitol, 0.1 mmol/L Na_3HO_4, 10 mmol/L $MgCl_2$) supplemented with 200 μmol/L ATP for 1

hour at 30°C. After three washes with lysis buffer the plate was incubated with the phospho-c-Jun (Ser63) antibody (rabbit polyclonal antibody against the phosphorylated fusion protein, 1:1000; Cell Signaling) for 1hour in blocking buffer (TBS with 0.1% Tween-20, with 2% fetal bovine serum). After three washes with TBS supplemented with 0.1% Tween-20, the plate was incubated with a secondary anti-rabbit antibody conjugated with horseradish peroxidase in blocking buffer (TBS with 0.1% Tween-20, with 2% fetal bovine serum) for 1 hour at room temperature. The plate was subsequently washed three times and the peroxidase reaction was developed and measured at 450 nm with a reference wavelength at 620 nm.

In Situ *Hybridization for VEGF*

Paraffin sections from formalin-fixed and diethyl pyrocarbonate-treated rat eyes, 4 μm thick, were dewaxed in xylene, rehydrated in decreasing ethanol concentrations, air-dried. and treated by sequential incubation as follows: 0.2 N HCL (20 minutes), double-distilled water (5 minutes), 0.125 mg/ml pronase (Roche Diagnostics), 0.02 mol/L glycine (30 seconds, Sigma), twice PBS (30 seconds). Specimens were postfixed in 4% paraformaldehyde/PBS for 20 minutes and washed in PBS (5 minutes). After incubation in 0.1 mol/L triethanolamine, pH 8.0, containing freshly added 0.25 vol % acetic anhydride for 10 minutes and dehydration in serial alcohols the sections were air-dried. The samples were incubated in a humid chamber for 2 hours at 42°C with prehybridization buffer (50% deionized formamide, 0.3 mol/L NaCl, 10 mmol/L Tris, pH 7.5, 10 mmol/L Na_2HPO_4, pH 6.8, 5 mmol/L EDTA, 0.1× Denhardt's solution, 10 mmol/L dithiothreitol, 0.25 mg/ml yeast tRNA, 12.5% dextransulfate, and 0.5 mg/ml salmon sperm DNA. For hybridization, prehybridization mix was removed and slides were covered with 30 μl of hybridization solution, containing 1 μg of digoxigenin-labeled cDNA probe/ml, and incubated for 18 hours at 42°C.

Retinal Leukocyte Adhesion Quantification

Retinal leukostasis was quantified as previously described[44] in diabetic rats treated with the above-described inhibitors, 2 weeks after the onset of diabetes. The total number of adherent leukocytes per retina was counted.

Statistical Analysis

All results are expressed as means ± SD. The data were compared by one-way analysis of variance and Duncan's posthoc test. Differences were considered statistically significant when the *P* values were less than 0.05.

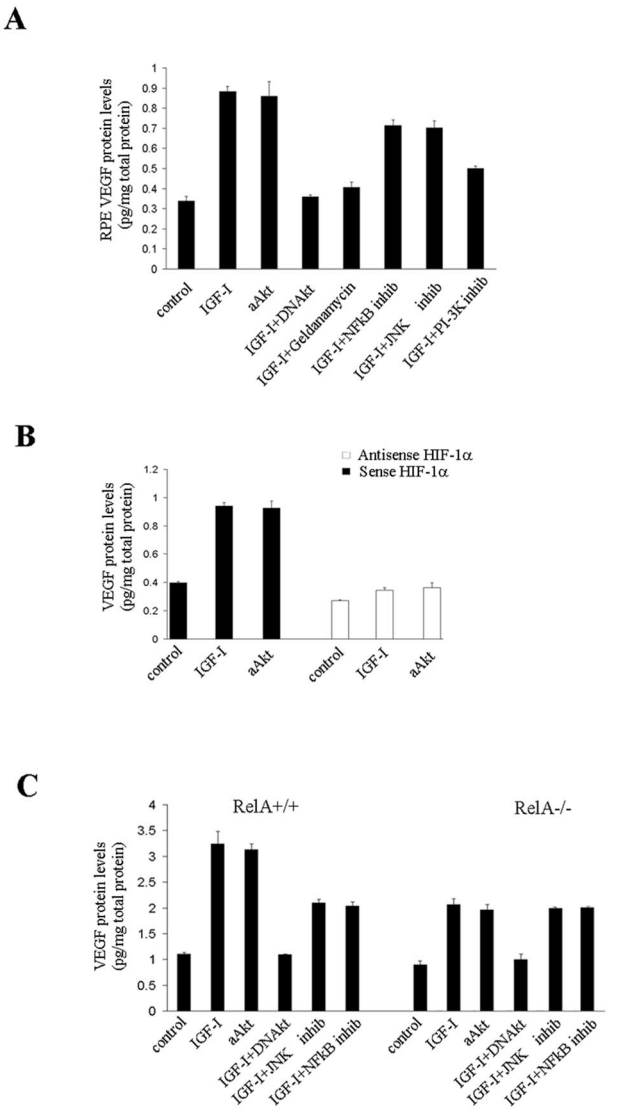

Figure 1. IGF-I up-regulates VEGF protein levels *in vitro*, through a PI-3K/Akt- and NF-κB/AP1-dependent up-regulation of HIF-1α activity. **A:** IGF-I and transfection with construct for constitutively active Akt (aAkt) induce a significant increase in VEGF expression ($n = 6$, $P < 0.005$ and $P < 0.001$, respectively) in human RPE cells *in vitro*, which is decreased significantly by DN-Akt, PI-3K inhibitors, or geldanamycin ($n = 6$, $P < 0.001$, in all cases), and, to a lesser extent, by SN50 and JNK inhibitor II ($n = 6$, $P < 0.001$, in both cases). **B:** IGF-I and constitutively active Akt (aAkt) up-regulate VEGF expression in human RPE cells *in vitro* that is abrogated by transfection of anti-sense oligonucleotides for HIF-1α ($n = 4$, $P < 0.001$ in both cases), but not sense oligonucleotides. **C:** The increase in VEGF protein levels by IGF-I or constitutively active Akt is significantly less pronounced in NF-κB knockout fibroblasts ($RelA^{-/-}$), than in their wild-type counterparts ($n = 4$, $P < 0.005$). DN-Akt reduced the IGF-I-induced VEGF increase in both wild-type and $RelA^{-/-}$ fibroblasts ($n = 6$, $P < 0.001$, in both cases), but SN50 and JNK inhibitor II reduced the VEGF increase only in the wild-type fibroblasts ($n = 4$, $P < 0.005$).

Results

IGF-I Stimulates VEGF Expression through a PI-3K/Akt- and NF-κB/AP-1-Dependent Mechanism in Vitro

We investigated the effect of IGF-I on VEGF production in human RPE cells *in vitro* and studied the signaling pathway(s) mediating this effect. We found that VEGF levels in the supernatants of RPE cells were increased after IGF-I stimulation ($P < 0.005$), or after transfection of RPE cells with vector encoding constitutively activated (myristoylated) Akt (Figure 1A). The IGF-I-induced VEGF increases were abrogated by transfection with a construct for DN-Akt; by the PI-3K inhibitor wortmannin; the hsp90 molecular chaperone inhibitor geldanamycin (which down-reg-

ulates the intracellular levels of various kinases, including Akt); and, to a lesser extent, by SN50, a peptide inhibitor of NF-κB nuclear translocation, and by the JNK inhibitor SP600125 (JNK inhibitor II) (Figure 1A). The increase in VEGF levels by IGF-I stimulation or constitutively active Akt was abrogated by transfection with anti-sense (but not sense) HIF-1α oligonucleotides (Figure 1B), indicating a key role for HIF-1α in mediating the stimulatory effect of IGF-I/Akt on VEGF expression. In further support of the role of NF-κB on IGF-I-induced VEGF transcription, this increase was more pronounced in the supernatant of fibroblasts from wild-type (wt) mice than from RelA$^{-/-}$ littermates (3.2-fold higher VEGF levels in IGF-I-stimulated cells RelA$^{+/+}$ than their control RelA$^{+/+}$ cells *versus* 2.3-fold higher VEGF levels in IGF-I-stimulated cells RelA$^{-/-}$ than their control RelA$^{-/-}$ cells, $P < 0.05$). Similarly, overexpression of constitutively active Akt induced a more pronounced increase of VEGF levels in supernatants of wt fibroblasts than in RelA$^{-/-}$ counterparts (Figure 1C). Transfection of DN-Akt vector abrogated the IGF-I-induced VEGF up-regulation in both wild-type and RelA$^{-/-}$ fibroblasts. As expected, the SN50 peptide inhibitor of NF-κB decreased the IGF-I-induced VEGF up-regulation only in wt, but not in RelA$^{-/-}$ fibroblasts, confirming the specificity of the inhibitor and the involvement of the NF-κB pathway in regulation of VEGF expression. Interestingly, the JNK inhibitor II suppressed the IGF-I-induced up-regulation of VEGF only in the wt but not RelA$^{-/-}$ fibroblasts (Figure 1C).

IGF-I Up-Regulates VEGF Transcription through an Element Located 1 to 1.7 kb Upstream of the Initiation Site

To further delineate the mechanism of IGF-I-induced stimulation of VEGF expression, we transiently transfected RPE cells with reporter constructs containing various regions of the VEGF promoter (VEGFpr). IGF-I (100 ng/ml) stimulated the activity of the full-length (1.7 kb) VEGFpr, but this effect was strongly suppressed in the 1.0-kb and totally absent in the 0.8-kb, 0.5-kb, and 0.1-kb promoter fragments (Figure 2A). IGF-I had no effect on the control pT81-luc (Figure 2A). This step-by-step deletional mapping identified a 0.7-kb region (between 1.0 kb to 1.7 kb upstream of the initiation site) as the one responsible for the IGF-I-induced effect on VEGF expression. Because this region contains AP-1, NF-κB, and HIF-1α response elements,[45] we addressed the relative roles of these transcription factors in mediating the stimulatory effect of IGF-I on VEGFpr activity. The IGF-I-induced 1.7-kb VEGFpr activity in RPE cells was reproduced by forced expression of constitutively active Akt; was potently abrogated by geldanamycin, the PI-3K inhibitors wortmannin and LY294002 and forced expression of DN-Akt; and was modestly decreased by the NF-κB inhibitor SN50, and JNK inhibitor II, which inhibits AP-1 activity (Figure 2B). Importantly, anti-sense (but not sense) HIF-1α oligonucleotide treatment of RPE cells abrogated the up-regulation of 1.7-kb VEGFpr activity by either IGF-I or forced overexpression of constitutively active Akt, indicating an essential role of HIF-1α in IGF-I/Akt-induced VEGF up-regulation (Figure 2B). In all cases, the above treatments had no effect on the activity of the control pT81-luc plasmid. In addition, the stimulatory effect of IGF-I and constitutively active Akt on 1.7-kb VEGFpr activity was less pronounced in RelA$^{-/-}$ than in wt fibroblasts (Figure 2C). Collectively, these data suggest that IGF-I stimulates VEGF transcription through a pathway involving PI-3K, Akt, NF-κB, and JNK/AP-1.

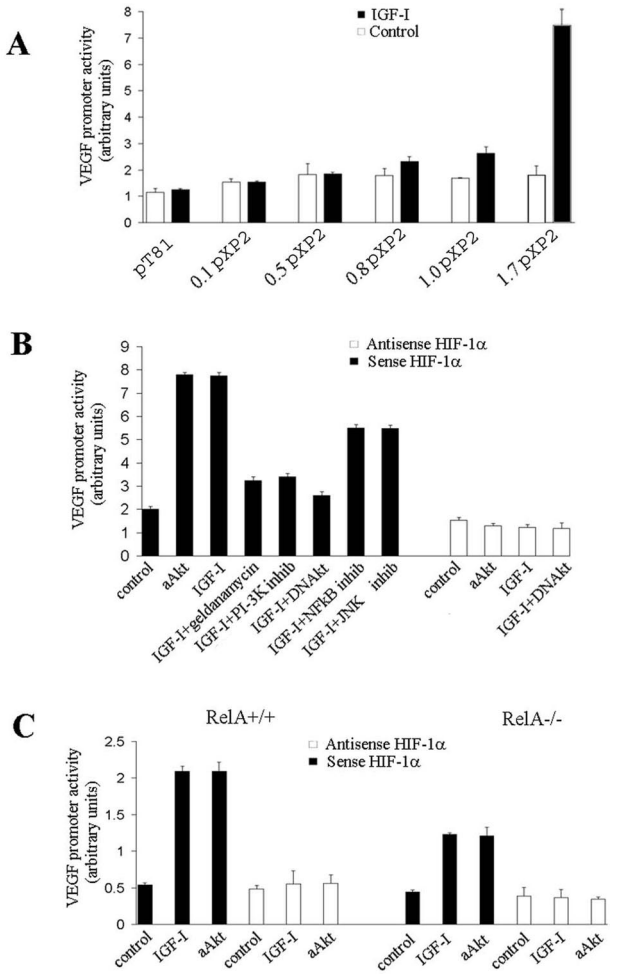

Figure 2. IGF-I up-regulates VEGF transcriptionally through an element located 1 to 1.7 kb upstream of the initiation site. **A:** IGF-I potently stimulated the VEGF promoter activity only in RPE cells transfected with the 1.7-kb VEGF promoter-luc plasmid ($n = 3$, $P < 0.001$), but had only a minor effect on the 1.0 pXP2 and no effect on the 0.8, 0.5, and 0.1 pXP2 VEGF promoter-luc plasmids or the control vector pT81-luc (pT81) ($n = 3$, $P > 0.05$, for the latter three plasmids). **B:** IGF-I and constitutively active Akt stimulated the 1.7-kb VEGF promoter-luc plasmid in RPE cells transfected with sense ($n = 3$, $P < 0.005$), but not in cells with anti-sense HIF-1α oligonucleotides ($n = 3$, $P > 0.05$). In cells transfected with sense HIF-1α oligonucleotides, the IGF-I-induced increase in VEGF promoter activity was significantly reduced by DN-Akt, geldanamycin, PI-3K inhibitors ($n = 3$, $P < 0.001$, in all three cases), and to lesser extent by the JNK inhibitor II and the NF-κB inhibitor SN50 ($n = 3$, $P < 0.0005$, in both cases), indicating a role for HIF-1α, NF-κB, and AP-1 in the IGF-I-stimulated VEGF up-regulation. **C:** The stimulation of 1.7-kb VEGF promoter-luc plasmid by IGF-I and constitutively active Akt was less pronounced in RelA$^{-/-}$ fibroblasts than their wild-type counterparts ($n = 3$, $P < 0.001$). Anti-sense oligonucleotides for HIF-1α abolished IGF-I or aAkt-induced up-regulation of 1.7-kb VEGFpr in both wt and RelA$^{-/-}$ fibroblasts ($n = 3$, $P < 0.001$, respectively), indicating the contribution of NF-κB to the Akt- and HIF-1α-dependent up-regulation of VEGF.

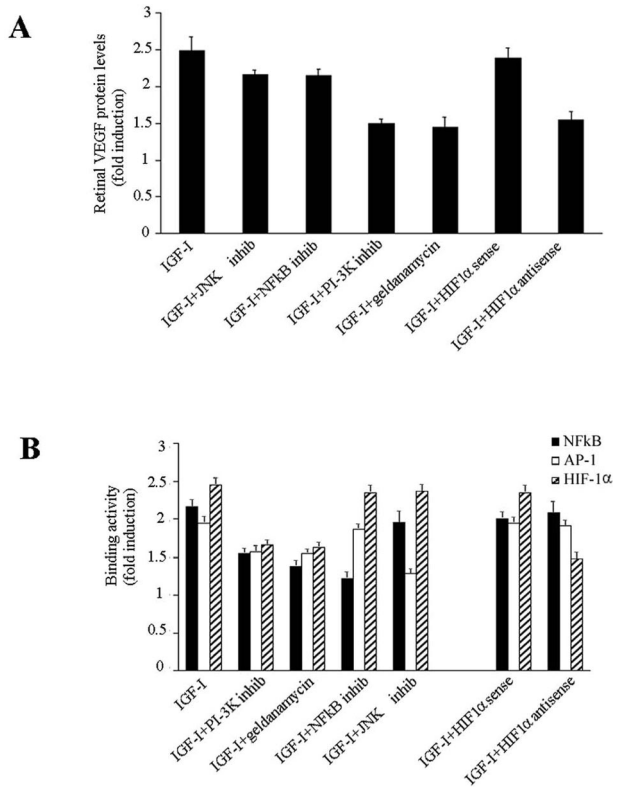

Figure 3. Intravitreal injection of IGF-I in the rat up-regulate VEGF through a NF-κB/AP-1- and PI-3-dependent up-regulation of HIF-1α. **A:** Intravitreal injection of IGF-I (50 ng) significantly increased retinal VEGF levels (2.48 ± 0.18-fold higher levels than in contralateral PBS-injected eyes, $n = 4$, $P < 0.002$). This increase was significantly suppressed by systemic administration of PI-3K inhibitors, geldanamycin and HIF-1α anti-sense (but not sense) oligonucleotides ($n = 8$, $P < 0.001$, in all cases), whereas JNK inhibitor II and SN50 had less pronounced inhibitory effect ($n = 8$, $P < 0.0002$ in both cases). **B:** Intravitreal injection of IGF-I (50 ng) up-regulates NF-κB, AP-1, and HIF-1α retinal activity (2.17 ± 0.14-, 1.94 ± 0.09-, and 2.45 ± 0.04-fold higher respective retinal activities than the contralateral PBS-injected eye, $n = 8$, $P < 0.0001$). These sequelae of IGF-I stimulation were significantly reduced by systemic administration of PI-3K inhibitors ($n = 4$, $P < 0.0002$ for each of the three transcription factors) and geldanamycin ($n = 8$, $P < 0.0003$ for each of the three transcription factors). JNK inhibitor II, SN50, and HIF-1α anti-sense oligonucleotides specifically inhibited the retinal activities of only AP-1 ($n = 7$, $P < 0.0001$), only NF-κB activity ($n = 6$, $P < 0.000001$), and only HIF-1α ($n = 7$, $P < 0.0001$), respectively.

IGF-I Stimulates VEGF Production in Vivo *through an NF-κB/AP-1- and HIF-1α-Dependent Pathway*

Intravitreous administration of IGF-I (50 ng) in Long-Evans rats increased retinal VEGF levels. Intraperitoneal administration (via osmotic pumps) of JNK inhibitor II, SN50, geldanamycin, and PI-3K inhibitors reduced the IGF-I-induced VEGF up-regulation. Moreover, intraperitoneal administration of a HIF-1α anti-sense oligonucleotide significantly reduced IGF-I-induced VEGF up-regulation (Figure 3A).

IGF-I Stimulates NF-κB, AP-1, and HIF-1α Activity in Vivo

Intravitreous injection of IGF-I (50 ng) induced significant increases in DNA-binding activity of NF-κB, AP-1, and HIF-1α from rat retina nuclear extracts (Figure 3B). These sequelae of IGF-I stimulation were significantly reduced by systemic administration of PI-3K inhibitors and geldanamycin. Systemic administration of SN50, JNK inhibitor II, or HIF-1α anti-sense oligonucleotides significantly attenuated the IGF-I-induced increase in the activity of only the respective transcription factors (NF-κB, AP-1, and HIF-1α, respectively). These data collectively delineate distinct signaling pathways that mediate the effect of IGF-I on VEGF promoter activity (Figure 3B).

HIF-1α Is Activated in Diabetic Retinas

HIF-1α binds to HREs in the VEGF promoter and up-regulates gene transcription *in vitro*.[25] We, therefore, investigated by electrophoretic mobility shift assay the binding of retinal nuclear extracts from nondiabetic and diabetic rats to biotin-labeled oligonucleotides containing sequences corresponding to the HRE and ancillary HRE sequences of the VEGF promoter. Nuclear extracts from diabetic retinae exhibited increased binding to the labeled oligonucleotides compared to nondiabetic controls. The pattern of binding demonstrated a constitutive slower migrating complex that increased on induction of diabetes; and a faster migrating complex evident only in the diabetic animals. Supershift assays confirmed that HIF-1α binding is present in the faster migrating complex, whereas the slower migrating complex consists of NF-κB and AP-1 heterodimers (Figure 4A). Quantification of the DNA-binding activity of HIF-1α in rat retinal nuclear extracts documented activity on induction of diabetes. Exogenous addition of a competitor (an oligonucleotide corresponding to the HIF-1α-binding element from the VEGF promoter) reduced HIF-1α DNA-binding activity, as measured *in vitro* by an ELISA-based assay, both in the nondiabetic and in the diabetic animals, confirming the specificity of the assay. Interestingly, AP-1 and NF-κB competitors (ie, oligonucleotides corresponding to respective DNA-binding sequences) inhibited by a lesser degree the levels of HIF-1α activation and only in the diabetic animals, whereas they had no effect in the nondiabetic animals. This suggested the possible presence of cooperation between HIF-1α and NF-κB/AP-1 in their binding to DNA (Figure 4B).

IGF-I Increases Early During the Course of Diabetic Retinopathy

IGF-I levels in rat retinae increased on the induction of diabetes (0.194 ± 0.055 pg/μg *versus* 0.091 ± 0.016 pg/μg of total retinal protein in the nondiabetic animals, $n = 7$, $P < 0.01$). Treatment with PI-3K inhibitors, geldanamycin, SN50, or JNK inhibitor II did not affect IGF-I levels in diabetic animals ($P > 0.05$) (Figure 5A).

JNK and Akt Activities Are Up-Regulated Early During the Course of Diabetic Retinopathy

JNK and Akt kinase activities were significantly increased on induction of diabetes (1.858 ± 0.117 and 2.3 ± 0.139

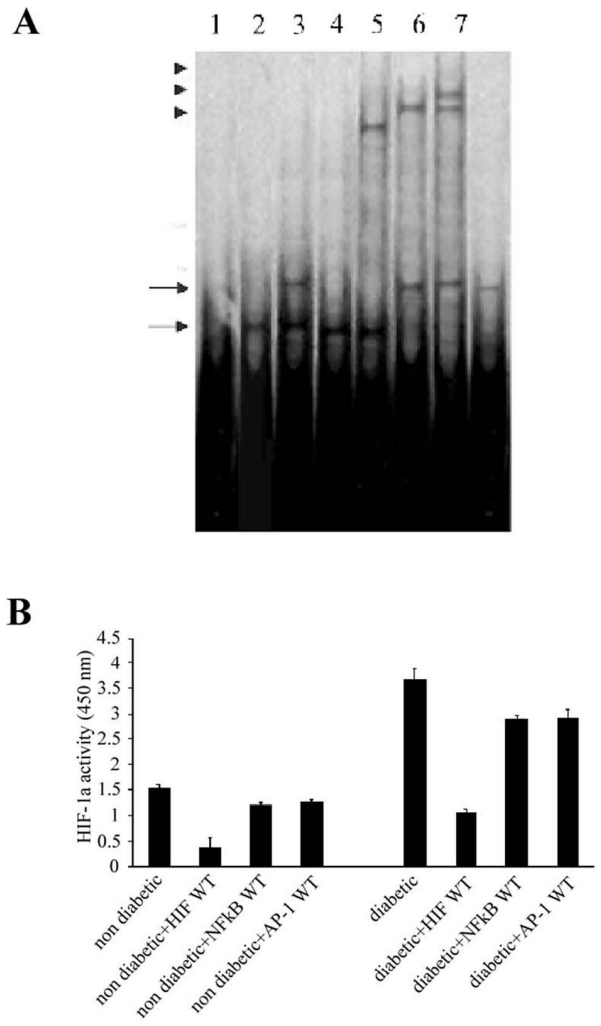

Figure 4. HIF-1a and NF-κB/AP-1 complexes transcriptionally regulate VEGF in the diabetic retinas through direct binding to the VEGF promoter. **A:** Retinal VEGF is up-regulated in diabetes through HIF-1α and NF-κB/AP-1 complexes that bind to the VEGF promoter. Retinal nuclear extracts from nondiabetic animals (**lane 2**) exhibit only a faster migrating complex (**double arrow**), whereas extracts from diabetic animals (**lane 3**) exhibit increased levels of the faster migrating complex that is supershifted by NF-κB (**lane 6**) and AP-1 (**lane 7**) antibodies, and a unique slower migrating complex that is supershifted by HIF-1α antibodies (**lane 5**). Unlabeled HIF-1α oligonucleotides competed the faster migrating complex (**lane** 4), whereas unlabeled AP-1 competed the slower migrating complex (**lane 8**). (**Lane 1** is the control lane, corresponding to probe without nuclear extract.) **B:** Retinal HIF-1α activity, quantified by modified ELISA assay, is significantly increased in diabetic *versus* nondiabetic animals ($P < 0.0001$), and is suppressed in both settings by oligonucleotides containing wild-type HIF-1α DNA-binding sites ($n = 5$, $P < 0.001$, in both cases).

arbitrary units in diabetic animals *versus* 0.724 ± 0.03 and 0.97 ± 0.08 arbitrary units in nondiabetic animals for JNK and Akt, respectively; $n = 8$, $P < 0.0001$ in both cases). These increases were reduced on systemic administration of an IGFR-neutralizing antibody whereas an isotype-matched control antibody had no effect (1.017 ± 0.105 and 0.956 ± 0.09 arbitrary units in diabetic animals that received the IGF-neutralizing antibody *versus* 1.87 ± 0.11 and 2.28 ± 0.17 arbitrary units in diabetic animals that received the isotype-matched control antibody, for JNK and Akt, respectively; $n = 8$, $P < 0.0001$ for JNK and $n = 7$, $P < 0.001$ for Akt activity). PI-3 kinase inhibition reduced both JNK and Akt activation during the course of diabetic retinopathy (1.21 ± 0.18 and 2.28 ± 0.17 arbitrary units in the diabetic animals that received the PI-3 inhibitors *versus* 1.858 ± 0.11 and 2.28 ± 0.17 arbitrary units in the diabetic animals that received the vehicle for JNK and Akt, respectively; $n = 6$, $P < 0.001$ for JNK and $n = 3$, $P < 0.0001$ for Akt activity). Likewise, administration of the hsp 90 inhibitor geldanamycin reduced significantly both JNK and Akt activity (0.81 ± 0.07 and 1.03 ± 0.15 arbitrary units in the diabetic animals that received geldanamycin *versus* 1.858 ± 0.11 and 2.28 ± 0.17 arbitrary units in the diabetic animals that received the vehicle for JNK and Akt, respectively; $n = 6$, $P < 0.001$ in terms of both JNK and Akt activity). JNK inhibitors suppressed mainly the increased JNK activity in diabetic retinas (0.937 ± 0.056 *versus* 1.858 ± 0.11 in the diabetic animals that received the JNK inhibitors *versus* the vehicle, $n = 6$, $P < 0.001$), whereas they had almost no effect in the Akt activation (2.032 ± 0.156 *versus* 2.28 ± 0.17 in the diabetic animals that received the JNK inhibitors *versus* the vehicle, $n = 6$, $P > 0.05$). Administration of the NF-κB inhibitor SN50 did not have a significant effect on JNK or Akt activation (1.745 ± 0.15 *versus* 1.858 ± 0.11 in the diabetic animals that received the SN50 for JNK, $n = 5$, $P > 0.05$ and 2.146 ± 0.154 *versus* 2.28 ± 0.17 in the diabetic animals that received the SN50 for Akt activation, $n = 5$, $P > 0.05$).

Neutralization of IGF-I Receptor or Its Downstream Signaling Effectors Reduces the Activity of Akt, JNK, NF-κB, HIF-1α, and AP-1 and Reduces Retinal VEGF Levels in a Rat Model of Diabetic Retinopathy

JNK and Akt activities in retinal extracts were significantly increased on induction of diabetes. These increases were reduced on systemic administration of an IGFR-neutralizing antibody (but not its isotype-matched antibody), PI-3K inhibitors, or geldanamycin. JNK inhibitors suppressed mainly the increased JNK activity in diabetic retinas, whereas SN50 had modest inhibitory effect, predominantly on JNK activation and less so on Akt activation (Figure 5B).

Moreover, consistent with our previous report,[3] retinal NF-κB activity was significantly increased on the induction of diabetes (Figure 5C). In the present study, this effect was attenuated with an IGFR-neutralizing antibody (but not its isotype-matched control), PI-3K inhibitors, geldanamycin, or SN50 (Figure 5C). Retinal AP-1 activity was also increased on the induction of diabetes ($P < 0.0001$) and this effect was attenuated with the IGFR-neutralizing antibody, PI-3K inhibitors, geldanamycin, JNK inhibitor II, and SN50 (all $P < 0.001$) (Figure 5C). Retinal HIF-1α activity increased on the induction of diabetes ($P < 0.001$) and this effect was significantly inhibited by systemic administration of IGFR-neutralizing antibody, PI-3K inhibitors, or geldanamycin (Figure 5C). The induction of diabetes in this model of diabetic retinopathy is characterized by a significant increase in retinal VEGF levels, which are blocked by systemic administration

of the IGFR-neutralizing antibody, PI-3K inhibitors, or geldanamycin, whereas inhibitors of JNK or NF-κB had a less potent inhibitory effect (Figure 5D).

VEGF, HIF-1α, and Phosphorylated Akt Demonstrate Similar Patterns of Distribution in a Rat Model of Diabetic Retinopathy

As previously described, VEGF mRNA levels increase on the induction of diabetes.[7,43,46] *In situ* hybridization for VEGF revealed no signal in control nondiabetic rats (Figure 6A), but intense cytoplasmic signal in the ganglion cell layer and inner nuclear layer of diabetic retinas (Figure 6B), whereas diabetic rats receiving IGFR-neutralizing antibody showed diminished signal (Figure 6C). Sections from diabetic rats hybridized with the sense probe did not show any signal (not shown). Immunohistochemistry for the active (phosphorylated) form of Akt (Figure 6; D to F), and for HIF-1α (Figure 6; G to I) showed similar tissue distribution; active Akt was localized in the cytoplasm, and HIF-1α in the nuclei (Figure 6, E and H, respectively) of the ganglion cell layer and the inner nuclear layer of diabetic rat retinas where glial and Mueller cells reside. Diabetic animals treated with the anti-IGF-1R-neutralizing antibody showed markedly diminished staining for VEGF, HIF-1α, and active Akt (Figure 6; C, F, and I, respectively).

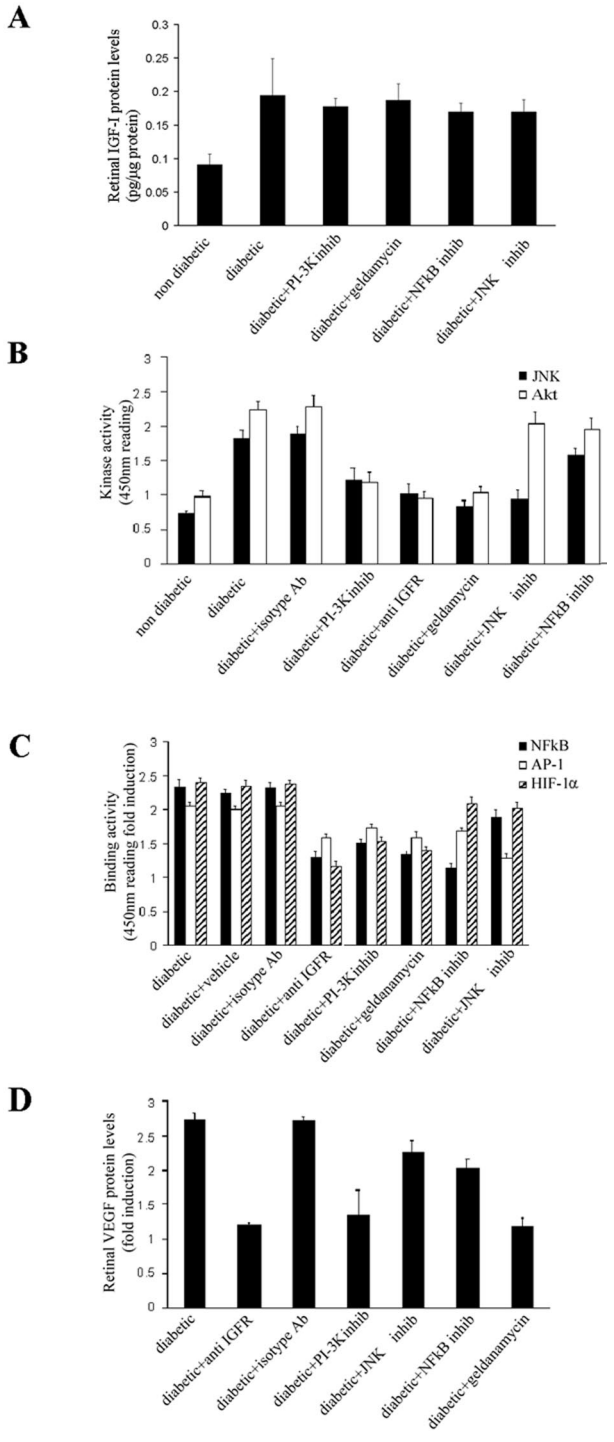

Figure 5. A: Retinal IGF-I levels increase on induction of diabetes (2.13 ± 0.08-fold induction over nondiabetic animals). This increase was not blocked by administration of geldanamycin or by inhibitors of either PI-3K, NF-κB, or JNK ($n = 7$, $P > 0.05$ in all cases). **B:** JNK and Akt activities were significantly increased on induction of diabetes ($n = 8$, $P < 0.0001$ in both cases). These increases were reduced on systemic administration of an IGFR-neutralizing antibody (not its isotype-matched antibody) ($n = 8$, $P < 0.0001$ for JNK and $n = 7$, $P < 0.001$ for Akt activity, respectively), PI-3K inhibitors ($n = 6$, $P < 0.001$ for JNK and $n = 3$, $P < 0.0001$ for Akt activity, respectively) or geldanamycin ($n = 6$, $P < 0.001$ in terms of both JNK and Akt activity). JNK inhibitors suppressed mainly the increased JNK activity in diabetic retinas ($n = 6$, $P < 0.001$), whereas SN50 did not have a significant effect on either JNK or Akt activation ($n = 5$, $P > 0.05$). **C:** NF-κB, AP-1, and HIF-1α activities are significantly increased in diabetic retinas (with more than twofold higher activities than nondiabetic animals, $n = 8$, $P < 0.0001$, in all cases). The increased activities of these transcription factors were significantly suppressed by systemic administration of IGFR-neutralizing antibody (but not its isotype-matched control) ($n = 7$, $P < 0.001$, for each of the three transcription factors), PI-3K inhibitors ($n = 6$, $P < 0.0001$, for each of the three transcription factor) or geldanamycin ($n = 6$, $P < 0.0001$, for each of the three transcription factors). Systemic administration of JNK inhibitors or SN50 decreased AP-1 ($n = 6$, $P < 0.001$), but had no effect on diabetes-induced increase of HIF-1α activity. **D:** On induction of diabetes, retinal VEGF protein levels were significantly increased ($n = 8$, $P < 0.0001$). Administration of IGFR-neutralizing antibody, PI-3K inhibitors, or geldanamycin ($n = 8$, $P < 0.0001$ in all three cases) significantly reduced the increase of VEGF levels in diabetic retinas. The inhibitory effect of JNK inhibitor II or SN50 on diabetes-induced increased VEGF levels ($n = 8$, $P < 0.001$) was less pronounced.

Inhibition of IGF-I-Induced Signaling Decreases Cardinal in Vivo *Manifestations of Diabetic Retinopathy*

We then investigated the effect of IGF-IR neutralization or inhibition of its downstream signaling cascades on the blood-retinal barrier breakdown that occurs in the rat 1 week after the onset of diabetes. In our model, retinal-blood barrier permeability in diabetic retinas was more than twofold higher compared to nondiabetic controls. Diabetic blood-retinal barrier breakdown was significantly reduced via the systemic administration of the IGFR-neutralizing antibody, geldanamycin, and PI-3K inhibitors, whereas the NF-κB inhibitor SN50 had a modest inhibitory effect (Figure 7A). Furthermore, the increase in retinal ICAM-1 levels observed during the first week of diabetes was attenuated by geldanamycin, IGFR-neutralizing antibody, PI-3K inhibitor, and, to a lesser degree, by SN50 (Figure 7B). In addition, as previously observed,[2,44]

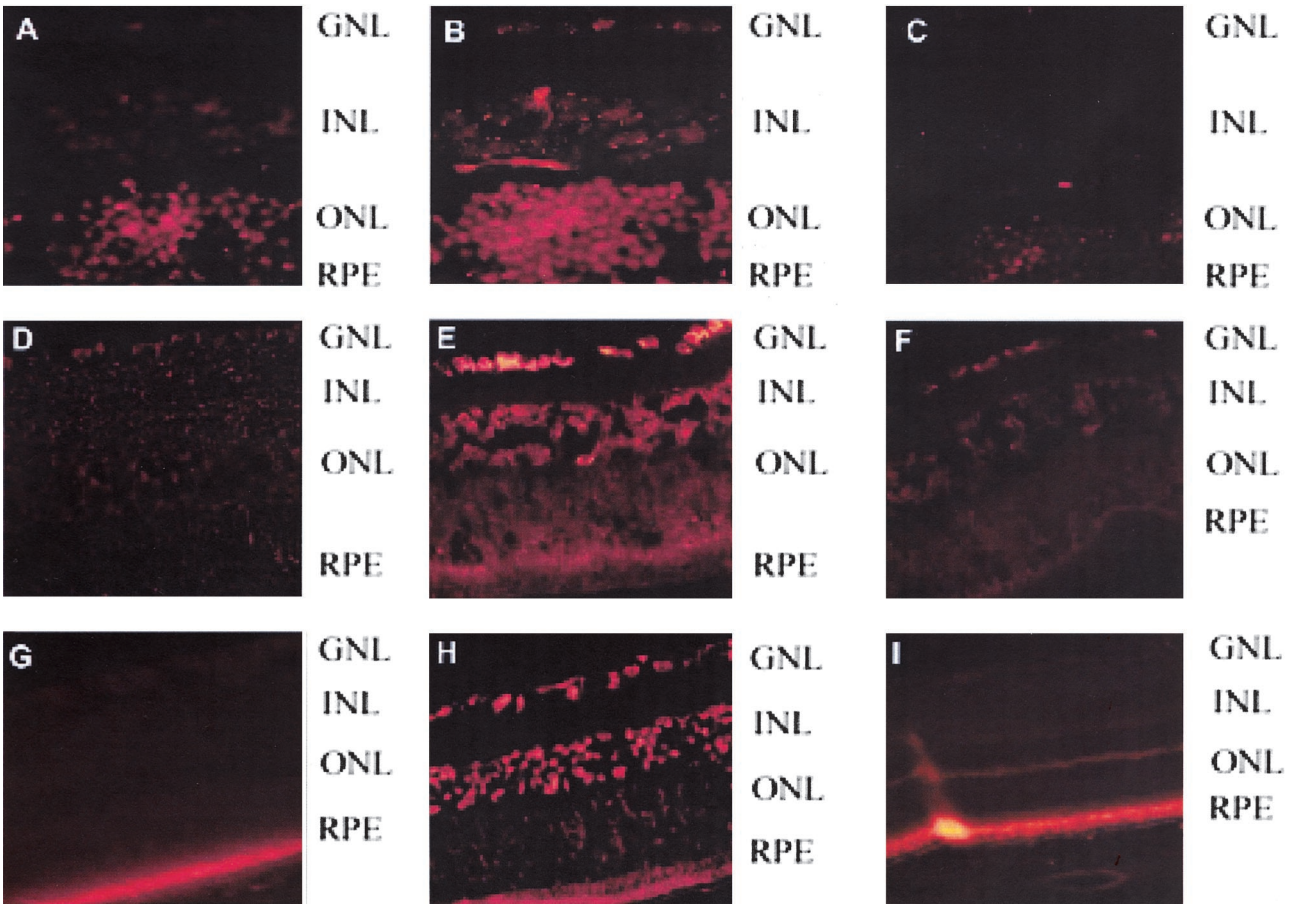

Figure 6. VEGF mRNA demonstrates similar patterns of distribution with HIF-1α and phosphorylated Akt proteins in the rat model of diabetic retinopathy. *In situ* hybridization for VEGF mRNA showed no staining in nondiabetic controls (**A**), in contrast to cytoplasmic staining in ganglion cell layer and inner nuclear layer of diabetic retinas (**B**). However, diabetic retinas of rats receiving systemic IGFR-neutralizing antibody showed diminished VEGF mRNA staining (**C**). The same cell types showed intense cytoplasmic staining for the activated form of Akt in diabetic rats (**E**), and significantly less staining in rats receiving IGFR-neutralizing antibody (**F**), whereas nondiabetic retinas (**D**) showed no staining. Retinas of nondiabetic rats (**G**) showed no nuclear staining for HIF-1α, but their diabetic counterparts (treated with isotype-matched control antibody) had intense staining for HIF-1α (**H**), whereas diabetic rats receiving systemic IGFR-neutralizing antibody showed less staining (**I**). The retinal layers are labeled as RPE, the RPE layer; INL, the inner nuclear layer; ONL, the outer nuclear layer; and GNL, the ganglion nuclear layer.

leukocyte adhesion in the diabetic retinas, causally related to blood-retinal barrier breakdown, was twofold higher 1 week after the onset of diabetes when compared to nondiabetic controls. The IGF-IR-neutralizing antibody, geldanamycin, and the PI-3K inhibitors (Figure 7C) attenuated the diabetes-associated increases in leukocyte adhesion.

Discussion

We previously demonstrated that deregulated VEGF expression plays a pivotal role in the induction of diabetic retinopathy in a relevant animal model by triggering inflammatory phenomena, such as adhesion molecule expression, leukocyte adhesion, endothelial dysfunction, and blood-retinal barrier breakdown.[3] We now document that IGF-I is a key, direct regulator of VEGF levels and blood-retinal barrier breakdown in early diabetic retinopathy. We also characterized the molecular pathways mediating these biological sequelae of IGF-I, and, in particular, the role of PI-3K/Akt-dependent activation of HIF-1α, NF-κB, and AP-1. Importantly, we found that inhibition of IGF-I-induced signaling cascades reduces retinal VEGF and ICAM-1 levels, leukocyte adhesion, and blood-retinal barrier breakdown.

Our finding of increased vitreous IGF-I levels on the onset of diabetes in rats suggests a possible role of IGF-I in the progression of diabetic retinopathy. Several studies have indicated an association between IGF-I levels and progression of diabetic retinopathy.[47–49] Exogenous IGF-I, as part of IGF-I replacement therapy, can have detrimental effects in the retinal circulation of humans and can cause blood-retinal barrier breakdown.[27] However, direct causal evidence regarding the role of IGF-I in diabetic retinopathy, beyond the above-mentioned associations, was still lacking. Moreover, the signaling pathway(s) downstream of the IGF-I receptor, as well as the identity of its effectors, had not been characterized. We now demonstrate not only that inhibition of IGF-I signaling can potently inhibit cardinal pathophysiological manifestations of diabetic retinopathy, such as the increased VEGF levels, blood-retinal barrier breakdown, and leuko-

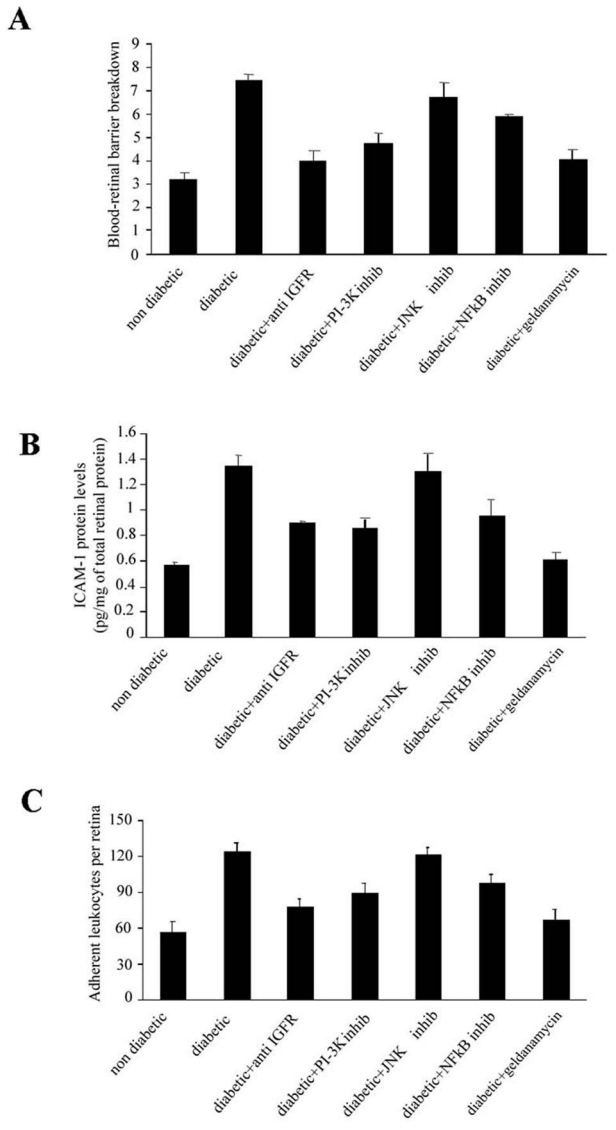

Figure 7. Inhibition of IGF-I-induced signaling decreases cardinal *in vivo* manifestations of diabetic retinopathy. **A:** The increase of blood-barrier breakdown in diabetic *versus* nondiabetic retinas ($n = 8$, $P < 0.001$) was significantly suppressed by systemic administration of anti-IGF-1R-neutralizing antibody (the isotype-matched control antibody had no effect; not shown) ($n = 10$, $P < 0.001$), PI-3K inhibitors ($n = 10$, $P < 0.005$), or geldanamycin ($n = 10$, $P < 0.001$). The NF-κB inhibitor SN50 had a less pronounced inhibitory effect on blood-barrier breakdown ($n = 8$, $P < 0.001$). **B:** The increase of retinal ICAM-1 levels in diabetic *versus* nondiabetic retinas ($n = 8$, $P < 0.001$) was significantly suppressed by systemic administration of anti-IGF-1R-neutralizing antibody (the isotype-matched control antibody had no effect; not shown) ($n = 8$, $P < 0.0002$), PI-3K inhibitors ($n = 8$, $P < 0.001$), geldanamycin ($n = 8$, $P < 0.001$), or SN50 ($n = 8$, $P < 0.001$). **C:** Leukocyte adhesion was increased in diabetic (2 weeks after the induction of diabetes) *versus* nondiabetic control rats ($n = 8$, $P < 0.001$). This increase was significantly attenuated by systemic administration of anti-IGF-1R-neutralizing antibody (the isotype-matched control antibody had no effect; not shown) ($n = 8$, $P < 0.0001$), PI-3K inhibitors ($n = 8$, $P < 0.0001$), geldanamycin ($n = 8$, $P < 0.0001$), or SN50 ($n = 8$, $P < 0.05$).

cyte adhesion, but also that the neutralization of the biological sequelae of IGF-I can occur by strategies targeting a variety of its multiple molecular effectors, including its cell-surface receptor and its downstream intracellular signaling mediators.

In support of our hypothesis, intravitreous administration of IGF-I increased leukostasis and vascular leakage in the rat retina (data not shown). It was recently reported that, in breast cancer cells, IGF-I induces the phosphorylation of ZO-1, a scaffolding protein that resides in the tight junctions.[50] In the vasculature, hyperphosphorylation of ZO-1 usually coincides with its departure from the tight junctions into the cytoplasm and with increased vascular permeability.[51] In addition, IGF-I may also lead to increased permeability via the up-regulation of VEGF. We have recently reported that leukocyte-endothelium interactions play an important role in blood-retinal breakdown in diabetes and that VEGF orchestrates this interaction by up-regulating the expression of adhesion molecules, in particular ICAM-1, in endothelial cells via the PI-3K/Akt/NO pathway.[43] Vitreous IGF-I levels are increased in diabetic retinopathy.[26] In agreement, we now demonstrate that inhibition of IGF-I signaling down-regulates Akt activity and ICAM-1 expression, as well as the transcriptional activity of NF-κB, AP-1, and HIF-1α in our *in vivo* diabetic model.

The functional interplay of the above-mentioned factors is highlighted by the similarities in the pattern of spatial distribution of VEGF, active Akt, and HIF-1α in diabetic retinae and confirmed by the detailed analysis of the signaling cascade induced by IGF-I *in vivo* and *in vitro*. In particular, IGF-I stimulates, in both our models, via PI-3K/Akt, two downstream pathways, culminating in the activation of the NF-κB/AP-1 complex and HIF-1α, respectively. The degree of cross talk between these two pathways is still unclear and is the subject of future investigation. The pivotal role of the PI-3K/Akt pathway in our model is established by the stimulating effect of constitutively active Akt on VEGF expression *in vitro*, the suppressive effect of PI-3K inhibition and DN-Akt on IGF-I-induced expression of VEGF in RPE cells *in vitro*, and by the suppressive effect of PI-3K inhibition on diabetes-induced retinal VEGF levels *in vivo*. The direct correlation of HIF-1α levels with VEGF levels on the inhibition of the above-mentioned kinases suggests that IGF-I regulates VEGF expression in the retina through the PI-3K/Akt-mediated induction of HIF-1α. This result was confirmed by deletional mapping of the promoter activity of VEGF in RPE cells and the inhibitory effect of HIF-1α anti-sense oligonucleotide, and correlates with our previous findings of induction of HIF-1α by insulin through a PI-3K- and p38 MAPK-dependent pathway.[38] Inhibition of the NF-κB/AP1 complex also attenuated VEGF expression, without affecting the levels of HIF-1α. In agreement with a role for NF-κB in the regulation of VEGF expression, IGF induced VEGF less efficiently in $Rel^{-/-}$ fibroblasts than in wild-type controls. Inhibition of PI-3K by wortmannin partially inhibited NF-κB activity. NF-κB activity has been found to be dependent on the activation of PI-3K and MAPK in several other systems.[52] It is interesting to note that PI-3K inhibition in our model resulted in the inhibition of JNK, probably explaining the inhibition of the AP-1 complex. Yet, JNK inhibition reduced VEGF expression without affecting significantly the activity of Akt, NF-κB, and HIF-1α activation *in vitro* after IGF-I treatment or *in vivo* on the induction of diabetes. These results delineate distinct signaling pathways for the regulation of VEGF expression in diabetic retinopathy. Yet, optimal transcriptional up-

regulation of the VEGF gene apparently requires coordinated activation of all three factors: NF-κB, AP-1, and HIF-1α, as evidenced by the at least partial blocking effect exerted on VEGF expression by pathway-specific inhibitors (SN50, JNK inhibitors, and HIF-1α anti-sense oligonucleotide, respectively). Indirect evidence for cooperation between these factors arises from the fact that, in Rel$^{-/-}$ fibroblasts, the partial suppression of IGF-induced activation of VEGF expression is not further potentiated by JNK inhibitors (suggesting that the effect of AP-1 requires the presence of NF-κB) and by our finding that the DNA-binding activity of HIF-1α in rat retinal nuclear extracts is partially attenuated by oligonucleotides corresponding to AP-1 and NF-κB DNA-binding sequences.

Although the rats used in our study had been diabetic only for 2 weeks, additional studies in our laboratory have demonstrated that similar pathophysiological mechanisms mediate the induction of retinal lesions in long-term diabetic animals,[53] thus confirming the validity of our model. Our findings, therefore, lead to clinically important conclusions about the pathogenesis of diabetic retinopathy and propose targets for pharmacological intervention. These data suggest that compounds inhibiting the activity of the IGF-I receptor or its downstream intracellular signaling pathways (eg, inhibitors of PI-3K or Akt) may correspond to novel therapeutic agents for this disease. In our study, geldanamycin, the prototypic member of the family of ansamycins, lowered Akt and JNK enzymatic activity, VEGF levels, and vascular leakage. Geldanamycin and its analogs inhibit the hsp90 molecular chaperone, leading to depletion of several kinases, including Akt (Mitsiades CS, Mitsiades N, McMullan CJ, Poulaki V, Kung AL, Davies FE, Dring A, Morgan G, Akiyama M, Shringapure R, Munshi N, Hideshima T, Chauhan D, Gu X, Bailey C, Joseph M, Libermann TA, Rosen NS, Anderson KC, manuscript in preparation).[54] Because of its pleiotropic effects, geldanamycin cannot be considered a specific Akt inhibitor. However, the value of these studies is the identification of a clinically applicable inhibitor of angiogenic signaling with possible use in the treatment of diabetic retinopathy, because geldanamycin analogs are currently undergoing clinical evaluation as inhibitors of growth factor-induced signaling in neoplastic diseases and have demonstrated a favorable pharmacological profile.[55]

In conclusion, we have characterized the important role of IGF-I in the pathogenesis of diabetic retinopathy and described its downstream signaling pathway(s), which involves the stimulation of VEGF gene expression through HIF-1α and NF-κB/AP-1. Inhibitors of the IGF-I receptor or its downstream effectors, such as Akt, NF-κB, and AP-1 represent potential novel pharmacological agents for the treatment of diabetic retinopathy.

Acknowledgments

We thank Dr. Andrew P. Levy and Dr. Mark A. Goldberg (Harvard Medical School, Boston, MA) for the generous gift of the VEGF promoter reporter plasmid and its deletion mutants.

References

1. Brinchmann-Hansen O, Dahl-Jorgensen K, Sandvik L, Hanssen KF: Blood glucose concentrations and progression of diabetic retinopathy: the seven year results of the Oslo study. BMJ 1992, 304:19–22
2. Miyamoto K, Khosrof S, Bursell SE, Rohan R, Murata T, Clermont AC, Aiello LP, Ogura Y, Adamis AP: Prevention of leukostasis and vascular leakage in streptozotocin-induced diabetic retinopathy via intercellular adhesion molecule-1 inhibition. Proc Natl Acad Sci USA 1999, 96:10836–10841
3. Joussen AM, Poulaki V, Mitsiades N, Kirchhof B, Koizumi K, Dohmen S, Adamis AP: Nonsteroidal anti-inflammatory drugs prevent early diabetic retinopathy via TNF-alpha suppression. EMBO J 2002, 16: 438–440
4. Adamis AP: Is diabetic retinopathy an inflammatory disease? Br J Ophthalmol 2002, 86:363–365
5. Aiello LP, Avery RL, Arrigg PG, Keyt BA, Jampel HD, Shah ST, Pasquale LR, Thieme H, Iwamoto MA, Park JE, Nguyen HV, Aiello LM, Ferrara N, King GL: Vascular endothelial growth factor in ocular fluid of patients with diabetic retinopathy and other retinal disorders. N Engl J Med 1994, 331:1480–1487
6. Aiello LP, Wong JS: Role of vascular endothelial growth factor in diabetic vascular complications. Kidney Int Suppl 2000, 77:S113–S119
7. Qaum T, Xu Q, Joussen AM, Clemens MW, Qin W, Miyamoto K, Hassessian H, Wiegand SJ, Rudge J, Yancopoulos GD, Adamis AP: VEGF-initiated blood-retinal barrier breakdown in early diabetes. Invest Ophthalmol Vis Sci 2001, 42:2408–2413
8. Miller JW, Adamis AP, Shima DT, D'Amore PA, Moulton RS, O'Reilly MS, Folkman J, Dvorak HF, Brown LF, Berse B: Vascular endothelial growth factor/vascular permeability factor is temporally and spatially correlated with ocular angiogenesis in a primate model. Am J Pathol 1994, 145:574–584
9. Tolentino MJ, Miller JW, Gragoudas ES, Chatzistefanou K, Ferrara N, Adamis AP: Vascular endothelial growth factor is sufficient to produce iris neovascularization and neovascular glaucoma in a nonhuman primate. Arch Ophthalmol 1996, 114:964–970
10. Adamis AP, Miller JW, Bernal MT, D'Amico DJ, Folkman J, Yeo TK, Yeo KT: Increased vascular endothelial growth factor levels in the vitreous of eyes with proliferative diabetic retinopathy. Am J Ophthalmol 1994, 118:445–450
11. Adamis AP, Shima DT, Tolentino MJ, Gragoudas ES, Ferrara N, Folkman J, D'Amore PA, Miller JW: Inhibition of vascular endothelial growth factor prevents retinal ischemia-associated iris neovascularization in a nonhuman primate. Arch Ophthalmol 1996, 114:66–71
12. Malecaze F, Clamens S, Simorre-Pinatel V, Mathis A, Chollet P, Favard C, Bayard F, Plouet J: Detection of vascular endothelial growth factor messenger RNA and vascular endothelial growth factor-like activity in proliferative diabetic retinopathy. Arch Ophthalmol 1994, 112:1476–1482
13. Murata T, Ishibashi T, Khalil A, Hata Y, Yoshikawa H, Inomata H: Vascular endothelial growth factor plays a role in hyperpermeability of diabetic retinal vessels. Ophthalmic Res 1995, 27:48–52
14. Aiello LP, Pierce EA, Foley ED, Takagi H, Chen H, Riddle L, Ferrara N, King GL, Smith LE: Suppression of retinal neovascularization in vivo by inhibition of vascular endothelial growth factor (VEGF) using soluble VEGF-receptor chimeric proteins. Proc Natl Acad Sci USA 1995, 92:10457–10461
15. Damert A, Ikeda E, Risau W: Activator-protein-1 binding potentiates the hypoxia-inducible factor-1-mediated hypoxia-induced transcriptional activation of vascular-endothelial growth factor expression in C6 glioma cells. Biochem J 1997, 327:419–423
16. Mukhopadhyay D, Tsiokas L, Sukhatme VP: Wild-type p53 and v-Src exert opposing influences on human vascular endothelial growth factor gene expression. Cancer Res 1995, 55:6161–6165
17. Shima DT, Kuroki M, Deutsch U, Ng YS, Adamis AP, D'Amore PA: The mouse gene for vascular endothelial growth factor. Genomic structure, definition of the transcriptional unit, and characterization of transcriptional and post-transcriptional regulatory sequences. J Biol Chem 1996, 271:3877–3883
18. Kuroki M, Voest EE, Amano S, Beerepoot LV, Takashima S, Tolentino M, Kim RY, Rohan RM, Colby KA, Yeo KT, Adamis AP: Reactive

oxygen intermediates increase vascular endothelial growth factor expression in vitro and in vivo. J Clin Invest 1996, 98:1667–1675
19. Pollenz RS, Sullivan HR, Holmes J, Necela B, Peterson RE: Isolation and expression of cDNAs from rainbow trout (Oncorhynchus mykiss) that encode two novel basic helix-loop-helix/PER-ARNT-SIM (bHLH/PAS) proteins with distinct functions in the presence of the aryl hydrocarbon receptor. Evidence for alternative mRNA splicing and dominant negative activity in the bHLH/PAS family. J Biol Chem 1996, 271:30886–30896
20. Jiang BH, Semenza GL, Bauer C, Marti HH: Hypoxia-inducible factor 1 levels vary exponentially over a physiologically relevant range of O2 tension. Am J Physiol 1996, 271:C1172–C1180
21. Wang GL, Jiang BH, Rue EA, Semenza GL: Hypoxia-inducible factor 1 is a basic-helix-loop-helix-PAS heterodimer regulated by cellular O2 tension. Proc Natl Acad Sci USA 1995, 92:5510–5514
22. Wang GL, Semenza GL: Purification and characterization of hypoxia-inducible factor 1. J Biol Chem 1995, 270:1230–1237
23. Guillemin K, Krasnow MA: The hypoxic response: huffing and HIFing. Cell 1997, 89:9–12
24. Levy AP, Levy NS, Wegner S, Goldberg MA: Transcriptional regulation of the rat vascular endothelial growth factor gene by hypoxia. J Biol Chem 1995, 270:13333–13340
25. Zelzer E, Levy Y, Kahana C, Shilo BZ, Rubinstein M, Cohen B: Insulin induces transcription of target genes through the hypoxia-inducible factor HIF-1alpha/ARNT. EMBO J 1998, 17:5085–5094
26. Meyer-Schwickerath R, Pfeiffer A, Blum WF, Freyberger H, Klein M, Losche C, Rollmann R, Schatz H: Vitreous levels of the insulin-like growth factors I and II, and the insulin-like growth factor binding proteins 2 and 3, increase in neovascular eye disease. Studies in nondiabetic and diabetic subjects. J Clin Invest 1993, 92:2620–2625
27. Danis RP, Bingaman DP: Insulin-like growth factor-1 retinal microangiopathy in the pig eye. Ophthalmology 1997, 104:1661–1669
28. Smith LE, Kopchick JJ, Chen W, Knapp J, Kinose F, Daley D, Foley E, Smith RG, Schaeffer JM: Essential role of growth hormone in ischemia-induced retinal neovascularization. Science 1997, 276:1706–1709
29. Poulsen JE: Diabetes and anterior pituitary insufficiency. Final course and postmortem study of a diabetic patient with Sheehan's syndrome. Diabetes 1966, 15:73–77
30. Luft R, Notter G: Preliminary results from treatment of juvenile diabetics with progressive vascular complications and neuropathy by implantation of the hypophysis with radioactive yttrium. Acta Isotopica 1964, 4:387–398
31. Merimee TJ: A follow-up study of vascular disease in growth-hormone-deficient dwarfs with diabetes. N Engl J Med 1978, 298:1217–1222
32. Simpson HL, Umpleby AM, Russell-Jones DL: Insulin-like growth factor-I and diabetes. A review. Growth Horm IGF Res 1998, 8:83–95
33. Jeffcoate W: Can growth hormone therapy cause diabetes? Lancet 2000, 355:589–590
34. Punglia RS, Lu M, Hsu J, Kuroki M, Tolentino MJ, Keough K, Levy AP, Levy NS, Goldberg MA, D'Amato RJ, Adamis AP: Regulation of vascular endothelial growth factor expression by insulin-like growth factor I. Diabetes 1997, 46:1619–1626
35. Lu M, Kuroki M, Amano S, Tolentino M, Keough K, Kim I, Bucala R, Adamis AP: Advanced glycation end products increase retinal vascular endothelial growth factor expression. J Clin Invest 1998, 101:1219–1224
36. Shima DT, Adamis AP, Ferrara N, Yeo KT, Yeo TK, Allende R, Folkman J, D'Amore PA: Hypoxic induction of endothelial cell growth factors in retinal cells: identification and characterization of vascular endothelial growth factor (VEGF) as the mitogen. Mol Med 1995, 1:182–193
37. Beg AA, Sha WC, Bronson RT, Ghosh S, Baltimore D: Embryonic lethality and liver degeneration in mice lacking the RelA component of NF-kappa B. Nature 1995, 376:167–170
38. Poulaki V, Qin W, Joussen AM, Hurlbut P, Wiegand SJ, Rudge J, Yancopoulos GD, Adamis AP: Acute intensive insulin therapy exacerbates diabetic blood-retinal barrier breakdown via hypoxia-inducible factor-1alpha and VEGF. J Clin Invest 2002, 109:805–815
39. Mitsiades CS, Mitsiades N, McMullan CJ, Poulaki V, Shringarpure R, Akiyama M, Hideshima T, Chauhan D, Joseph M, Libermann TA, Garcia-Echeverria C, Pearson MA, Hofmann F, Anderson KC, Kung AL: Inhibition of the insulin-like growth factor receptor-1 tyrosine kinase activity as a therapeutic strategy for multiple myeloma, other hematologic malignancies and solid tumors. Cancer Cell 2004, 5:221–230
40. Xu Q, Qaum T, Adamis AP: Sensitive blood-retinal barrier breakdown quantitation using Evans blue. Invest Ophthalmol Vis Sci 2001, 42:789–794
41. Mitsiades N, Mitsiades CS, Poulaki V, Chauhan D, Fanourakis G, Gu X, Bailey C, Joseph M, Libermann TA, Treon SP, Munshi NC, Richardson PG, Hideshima T, Anderson KC: Molecular sequelae of proteasome inhibition in human multiple myeloma cells. Proc Natl Acad Sci USA 2002, 99:14374–14379
42. Mitsiades N, Mitsiades CS, Poulaki V, Chauhan D, Richardson PG, Hideshima T, Munshi NC, Treon SP, Anderson KC: Apoptotic signaling induced by immunomodulatory thalidomide analogs in human multiple myeloma cells: therapeutic implications. Blood 2002, 99:4525–4530
43. Joussen AM, Poulaki V, Qin W, Kirchhof B, Mitsiades N, Wiegand SJ, Rudge J, Yancopoulos GD, Adamis AP: Retinal vascular endothelial growth factor induces intercellular adhesion molecule-1 and endothelial nitric oxide synthase expression and initiates early diabetic retinal leukocyte adhesion in vivo. Am J Pathol 2002, 160:501–509
44. Joussen AM, Murata T, Tsujikawa A, Kirchhof B, Bursell SE, Adamis AP: Leukocyte-mediated endothelial cell injury and death in the diabetic retina. Am J Pathol 2001, 158:147–152
45. Kimura H, Weisz A, Ogura T, Hitomi Y, Kurashima Y, Hashimoto K, D'Acquisto F, Makuuchi M, Esumi H: Identification of hypoxia-inducible factor 1 ancillary sequence and its function in vascular endothelial growth factor gene induction by hypoxia and nitric oxide. J Biol Chem 2001, 276:2292–2298
46. Joussen AM, Huang S, Poulaki V, Camphausen K, Beecken WD, Kirchhof B, Adamis AP: In vivo retinal gene expression in early diabetes. Invest Ophthalmol Vis Sci 2001, 42:3047–3057
47. Chantelau E, Seppel T, Althaus C, Schonau E: Elevation of serum IGF-1 rather than sex steroids precedes proliferative diabetic retinopathy in Mauriac's syndrome. Horm Res 1997, 48:131–134
48. Spoerri PE, Ellis EA, Tarnuzzer RW, Grant MB: Insulin-like growth factor: receptor and binding proteins in human retinal endothelial cell cultures of diabetic and non-diabetic origin. Growth Horm IGF Res 1998, 8:125–132
49. Burgos R, Mateo C, Canton A, Hernandez C, Mesa J, Simo R: Vitreous levels of IGF-I, IGF binding protein 1, and IGF binding protein 3 in proliferative diabetic retinopathy: a case-control study. Diabetes Care 2000, 23:80–83
50. Mauro L, Bartucci M, Morelli C, Ando S, Surmacz E: IGF-I receptor-induced cell-cell adhesion of MCF-7 breast cancer cells requires the expression of junction protein ZO-1. J Biol Chem 2001, 276:39892–39897
51. Antonetti DA, Barber AJ, Hollinger LA, Wolpert EB, Gardner TW: Vascular endothelial growth factor induces rapid phosphorylation of tight junction proteins occludin and zonula occluden 1. A potential mechanism for vascular permeability in diabetic retinopathy and tumors. J Biol Chem 1999, 274:23463–23467
52. Garcia-Garcia E, Sanchez-Mejorada G, Rosales C: Phosphatidylinositol 3-kinase and ERK are required for NF-kappaB activation but not for phagocytosis. J Leukoc Biol 2001, 70:649–658
53. Joussen AM, Poulaki V, Le ML, Koizumi K, Esser C, Janicki H, Schraermeyer U, Kociok N, Fauser S, Krohne TU, Kirchof B, Kern TS, Adamis AP: A central role for inflammation in the pathogenesis of diabetic retinopathy. FASEB J, in press
54. Basso AD, Solit DB, Munster PN, Rosen N: Ansamycin antibiotics inhibit Akt activation and cyclin D expression in breast cancer cells that overexpress HER2. Oncogene 2002, 21:1159–1166
55. Workman P, Maloney A: HSP90 as a new therapeutic target for cancer therapy: the story unfolds. Expert Opin Biol Ther 2002, 2:3–24